Feb 3rd, 2018

Lactic acid downregulates viral microRNA to promote Epstein-Barr Virus-immortalized B lymphoblastic cell adhesion and growth

Xiaohui Mo[14†], Fang Wei[2†], Yin Tong[3†], Ling Ding[1†], Qing Zhu[1†], Shujuan Du[1†], Fei Tan[4†], Caixia Zhu[1], Yuyan Wang[1], Qian Yu[4], Yeqiang Liu[5], Erle S Robertson[6], Zhenghong Yuan[1], Qiliang Cai[1#]

1 MOE& MOH Key Laboratory of Medical Molecular Virology, School of Basic Medicine, Shanghai Medical College, Fudan University, Shanghai 200032, P. R. China

2 ShengYushou Center of Cell Biology and Immunology, School of Life Sciences and Biotechnology, Shanghai Jiao Tong University, Shanghai 200240, P. R. China

3 Division of Hematology, Shanghai First People's Hospital, Shanghai Jiao Tong University, Shanghai 200080, P. R. China

4 Central *Laboratory, Shanghai Dermatology Hospital, Shanghai 200443, P. R. China.*

5 Division of Pathology, Shanghai Dermatology Hospital, Shanghai 200443, P. R. China.

6 Department of Microbiology, Perelman School of Medicine, University of Pennsylvania, Philadelphia 19104, United States of America

Running Title: LA induces LCL cell adhesion

†Equally contributed to this work.

Corresponding authors: QC (qiliang@fudan.edu.cn)

ABSTRACT

High plasma lactate is associated with poor prognosis of many malignancies, but its role in virally mediated cancer progression and underlying molecular mechanisms are unclear. Epstein–Barr virus (EBV), the first human oncogenic virus, causes several cancers, including B cell lymphoma. Here, we report that lactate dehydrogenase (LDH-A) expression and lactate production are elevated in EBV-immortalized B lymphoblastic cells, and lactic acid (LA, acidic lactate) at low concentration triggers EBV-infected B cell adhesion, morphological changes, and proliferation *in vitro* and *in vivo*. Moreover, LA-induced responses of EBV-infected B cells uniquely occurs in viral latency type III and it is dramatically associated with the inhibition of global viral microRNAs, particularly the miR-BHRF1 cluster, and the high expression of *SMAD3*, *JUN*, and *COL1A* genes. The introduction of miR-BHRF1-1 blocks the LA-induced effects of EBV-infected B cells. Thus, this may be a novel potential mechanism to explain EBV-immortalized B lymphoblastic cell malignancy in an LA microenvironment.

Key Words: Lactic Acid, EBV, B lymphoma, microRNA

43 **IMPORTANCE**

44 The tumor microenvironment is complicated, and lactate, which is created
45 by cell metabolism, contributes to an acidic microenvironment that facilitates
46 cancer progression. However, how lactic acid (LA) operates in
47 virus-associated cancers is unclear. Thus, we studied how the Epstein-Barr
48 virus (EBV, first tumor virus identified in humans; it is associated with many
49 cancers) upregulates the expression of lactate dehydrogenase (LDH-A) and
50 lactate production in B-lymphoma cells. Elevated LA induces adhesion and the
51 growth of EBV-infected B cells by inhibiting viral microRNA transcription. Thus,
52 we offer a novel understanding of how EBV utilizes an acidic
53 microenvironment to promote cancer development.

INTRODUCTION

Cancers can adopt distinctive metabolic strategies to sustain cell proliferation in a fluctuating microenvironment with variable oxygen and nutrient availability. Such metabolic reprogramming produces lactate even in the presence of oxygen, and is often referred as “aerobic glycolysis” or the “Warburg effect” (1). Growth factors, hypoxia, and oncogenes stimulate glycolysis and lactate production and subsequently induce the Warburg effect in either non-transformed or cancer cells (2). Considerable evidence indicates that lactate is not only a potent fuel source for aerobic metabolism, but it is also constantly produced and circulated throughout the body (3). In lactate-producing tissues or conditions, circulating lactate is taken up and oxidized as fuel by local and distant tissues and this cell-to-cell lactate shuttle can replace glucose as fuel for almost all types of cells (4). Recent studies suggest that lactate is a potent signaling molecule that promotes stabilization of hypoxia inducible factor-α (HIF-α), and increases VEGF expression and angiogenesis (5, 6).

The accumulation of lactate often leads to the formation of an LA microenvironment, and is frequently associated with cancer progression, increased metastasis, and poor disease-free and overall survival (7). LDH is widely expressed in different tissues and detectable in serum as it catalyzes the interconversion of pyruvate and lactate during glycolysis and gluconeogenesis. LDH catalysis is a rapid and near-equilibrium reaction that

relies heavily on local lactate gradients (8). Increased LDH and production of lactate are considered aspects of poor prognosis for several malignancies, including solid tumors (9, 10), but whether and how oncogenic viruses exploit this metabolic program to induce cancer development and respond to an acidic microenvironment is not clear.

Epstein-Barr Virus (EBV), the first oncogenic virus identified in humans, is a γ-herpes virus with global widespread distribution (latently infecting > 90% of adults for life) (11). In healthy individuals, EBV is controlled by the immune system and infections remain asymptomatic. In individuals with immune system suppression or dysfunction, the virus is reactivated and presents oncogenic potential *in vivo*, which is reflected in its ability to transform B-lymphocytes *in vitro*. EBV is associated with many human B- and T-lymphocytic and epithelial malignancies, including Burkitt's lymphoma, Hodgkin's disease, post-transplant lymphoma, diffuse large B cell lymphoma (DLBCL), and nasopharyngeal carcinoma (NPC) (11). According to the expression of viral latent genes, the status of EBV infection within host cancer cells are of three types of latency—I, II, and III—which could interconvert or directly reactivate to lytic replication (12). Among these, EBV-immortalized B lymphoblastic cells are referred to as latency III (13). Extensive studies focusing on EBV have accelerated our understanding of oncogenic mechanisms underlying EBV-driven B-cell oncogenesis (14). Evidence suggests that dynamic interactions between EBV and surrounding

98 microenvironmental factors (i.e., hypoxia stress) are significantly associated
99 with host cell malignant behavior (15-19). Although previous studies indicated
100 that EBV can activate anaerobic glycolysis for survival of NPC and B
101 lymphoma by up-regulating the expression of LMP1 and HIF-1α oncoproteins
102 (16, 20, 21), and LA promoted the growth of EBV-immortalized B cells in
103 serum-free conditions (22). However, whether and how EBV-driven host cells
104 respond to an acidic microenvironment is not clear.

105 In this study, we demonstrated that the expression of LDH-A and lactate
106 production are elevated in EBV-immortalized B lymphoblastic cells, and LA at
107 low concentrations induces cell adhesion, morphological changes, and
108 proliferation *in vitro* and *in vivo*. Functional bioinformatic analysis of differential
109 mRNA expression profiles revealed that genes relevant to metabolism and
110 environmental information processing are the most significantly and
111 specifically influenced in EBV-infected B cells' response to LA. In particular,
112 LA-induced effects of EBV-infected B cells were found to be associated with
113 viral latency III, and they were significantly associated with the inhibition of viral
114 microRNAs, particularly the expression of the genes *SMAD3* and *JUN*, which
115 are targeted by EBV-encoded miR-BHRF1-1. These results provide a
116 framework for the characterization of the molecular network involved in
117 interactions between an acidic microenvironment and EBV-coordinated
118 invasion.

MATERIALS AND METHODS

Cell culture — EBV-negative B-lymphoma cell lines (Ramos and BJAB from American Type Culture Collection [ATCC], Manassas, VA) and EBV-positive cell lines (B95.8 from ATCC and EBV-transformed primary B cell lines LCL *in vitro* generated in this study) were cultured in RPMI-1640 (Invitrogen) supplemented with 10% fetal bovine serum (FBS) (Hyclone), 100 U/ml penicillin and 100μg/ml streptomycin. HEK293 (from ATCC cells) grew in Dulbecco's modified Eagle's medium (Hyclone) with 10% FBS, 100 U/ml penicillin and 100μg/ml streptomycin. All cells were maintained at 37°C with 5% CO_2.

Plasmids and cell transfection — Plasmid DNAs were purified with TIANprep Mini Plasmid Kit (TIANGEN, China). The EBV-infected cells B95.8 and LCL were transfected with plasmid DNA or RNA oligonucleotide by using Entranster^{TM}-D4000 and R4000 reagent following the manufacturer's instruction (Engreen, Inc.). At 48-hours post transfection, the cells were harvested for qPCR and western blotting analyses. The miR-BHRF1-1 mimics (5'-UAA CCU GAU CAG CCC CGG AGUU-3') were synthesized (GenePharma, Shanghai). The miR-B1-1 inhibitor or nonspecific control oligonucleotide were individually synthesized and cloned into pGIPZ-basic vector for generating LCL cells stable expressing miR-BHRF1-1 inhibitor or control.

Analysis of extracellular lactate production — Two hundred thousand cells were seeded in 6-Well plates for 48 hr. The levels of lactic acid in cell culture supernatants were measured with a COBAS analyzer (Roche, Germany)

141 according to the manufacturer's instructions.

142 **Cell viability assay** — Cells were inoculated in a 96-well plate (100 μl per well,
143 6 repeated wells) in a density of 5×10^5 cell per ml. After treatment with different
144 concentration of lactic acid, cells were incubated for 24hr, and 20μl of
145 Methyl-thiazolyltetrazolium (MTT) solution (5 mg/ml, Sigma) were added into each
146 well. After 4hr incubation, the incubation was terminated, and the culture medium
147 was discarded. 150 μl DMSO was added to each well, and gently shaken for 10
148 min to promote crystallization dissolution. Absorbance values (OD) were
149 determined with an enzyme-linked immunosorbent detector.

150 **Quantitative PCR —** Total RNA was extracted with TRIzol reagent (Invitrogen),
151 complementary DNA (cDNA) was synthesized with the PrimeScript RT reagent Kit
152 (TaKaRa, Dalian). Quantitative PCR (qPCR) was performed in triplicate with
153 SYBR Premix ExTaq (TaKaRa, Dalian). The level of LDH-A was investigated by
154 qPCR. Quantification of EBV-miR-BHRF1-1 was conducted with TaqMan
155 microRNA assays (Genepharma, Shanghai). Mature miRNAs were reverse
156 transcribed, and quantitated by using All-in-One miRNA qPCR Detection Kit
157 following the manufacturer's protocol (Genepharma). U6 and GAPDH were used
158 for normalizing the expression of miRNA and mRNA, respectively. The fold
159 changes were calculated by using the $2^{-\Delta\Delta Ct}$ method. The primers used for
160 amplification of the interested genes were listed in Table 1.

161 **Cell adhesion and motility assays —** Equal amount EBV infected or uninfected
162 B cells were treated with 10mM lactic acid followed by photographed by

163 microscope at 24 hour for cell adhesion, or were real-time monitored by
164 xCELLIgence system (ACEA Biosciences, Inc.) for cell adhesion and proliferation.
165 Experiments were performed in triplicate with 2 repeats. For cell motility, 2×10^5
166 cells in 100 ml of serum-free RPMI-1640 media were triplicate seeded in each
167 fibronectin-coated polycarbonate membrane insert in a transwell apparatus
168 (Corning). 600 ml of 10% FBS in RPMI-1640 was added to the bottom chamber.
169 Cells were incubated at 37°C for 18 hr. The inserts were washed twice with
170 prewarmed PBS. Cells adhered on the lower surface were fixed with 100%
171 methanol at RT for 15 min and stained with hematoxylin for 15min. Cell numbers
172 were counted under the microscope. All assays were independently repeated at
173 least for three times. Cell invasion assays were performed as the migration assay
174 except the transwell membrane was precoated with 24 mg/ml Matrigel (R&D
175 Systems) and the cells were incubated for 24 hr, respectively.
176 **Immunoblotting —** Immunoblotting analyses were performed by using standard
177 methods. In brief, cells were harvested and lysed in the RIPA buffer containing
178 protease inhibitors (Sigma-Aldrich) and phosphatase inhibitors (Keygen, China).
179 Proteins were separated by SDS–polyacrylamide gel electrophoresis gels, and
180 blotted onto PVDF membrane (Millipore). The membrane was probed with the first
181 antibody as indicated and then with the peroxidase-conjugated secondary
182 antibody. SMAD3, JUN, COL1A, TGFBR1 and β-actin antibodies were purchased
183 from Santa Cruz Biotech. Inc.. Western blotting bands were visualized by ECL
184 Western Blot Kit (CWBIO Technology) and captured with ChemiDoc^{TM}XRS

Molecular Imager (Bio-Rad). All blots in figures were accompanied by the locations of molecular weight/size markers.

RNA-deep sequencing — RNA-deep sequencing was performed and analyzed in RiboBio (Ribobio Co. Ltd, Guangzhou, China). In brief, mRNAs were isolated from the DNase-treated total RNAs with the Dynabeads mRNA Purification Kit (Life Technologies). According to the manufacturer's instructions, the mRNAs were fragmented with divalent cations and converted to single-strand cDNA with random hexamer primers and Superscript II reverse transcriptase (Life Technologies). The second strand of cDNA was generated by RNase H (Enzymatics) and DNA polymerase. cDNA products were purified by Ampure beads XP (Beckman). After converting the overhangs into blunt ends using T4 DNA polymerase and Klenow DNA polymerase, extra 'A' base was added to the 3'-end of cDNA by Klenow enzyme. Sequencing adapters were then ligated to the end of cDNA by T4 DNA Ligase (Enzymatics). The fragments of 200 bp were selected by Ampure beads XP (Beckman) and enriched by 12 cycles of PCR. The PCR products were loaded into flowcell to generate clusters and then sequenced by Hiseq 2000 (Illumina).

Small RNA library construction and sequencing — Small RNA library construction and sequencing was performed by Ribobio Co. Ltd and followed the manufacturer's instructions. Briefly, small RNAs ranging from 18 to 30 nt were gel purified and ligated to the 3' adaptor and 5' adaptor. Ligation products were gel purified, reverse transcribed and amplified. The purified cDNA library was used for

cluster generation on Illumina's Cluster Station (San Diego, CA, USA) and subsequently sequenced on Illumina HiSeq 2500 (San Diego, CA, USA), following the manufacturer's instruction on running the instrument. Raw sequencing reads were obtained by using related Illumina's analysis software.

Prediction of miRNA targets — EBV-miRNA candidate targets were initially obtained from the RNA-deep sequencing in BGI-Shenzhen of China (Table 2) and then enriched with literature retrieval. The RNA-hybrid programme (http://bibiserv.techfak.uni-bielefeld.de/rnahybrid/sub mission.html) was used to predict duplex complementation between human SMAD3 3'-UTR, JUN 3'-UTR and EBV-miR-BHRF1-1.

Luciferase reporter assays — The MiTarget microRNA 3'-UTR target vector (pEZX-MT01) containing full-length 3'-UTR of SMAD3 or JUN with two binding sites for EBV-miR-BHRF1-1 (wild-type 3'-UTR) was constructed. The mutants of SMAD3 3'-UTR and JUN 3'-UTR were individually generated by site-directed mutagenesis by using KOD-Plus-Mutagenesis Kit (SMK-101, Toyobo C. Ltd). For luciferase reporter assays, Wild type (wt) or mutant (mut) of 3'-UTR vector was co-transfected with EBV-miR-BHRF1-1 mimic or nonspecific mimic control (Genepharma) into HEK 293 cells, respectively. Luciferase activity was measured at 48 hr post-transfection by using Luc-Pair miR Luciferase Assay Kit (GeneCopoeia) on Panomics Luminometer.

Statistical analysis — All experiments were performed in triplicate. Data shown are mean ±s.e.m. (unless otherwise specified) from at least three

independent experiments. SPSS 16.0 software was used for statistical analyses. Differences were considered to be statistically significant at values of $p<0.05$ by Student's *t*-test for two groups, one-way ANOVA (analysis of variance) analysis for multiple groups and parametric generalized linear model with random effects for tumour growth. Correlation was analyzed with two-tailed Spearman's correlation analysis. Single, double and triple asterisks individually indicate statistical significance* $p<0.05$, ** $p<0.01$ and *** $p<0.001$.

RESULTS

LDH-A and lactate production are elevated in EBV-immortalized B cells

To understand how EBV drives B-cell lymphoproliferative malignancy, we found that in normal LCL1 and LCL2 cells (Figure 1A, right), adhesive cells were consistent and had spindle-like morphological changes during the exponential growth of cells on culture day 5 (Figure 1B). We measured LDH-A and lactate expression in several EBV-infected (B95.8, LCL1, LCL2) and uninfected (Ramos, BJAB) B lymphoma cells and naïve B cells, after 24 h of culture. EBV-infected B cells had more LDH-A transcripts than the uninfected B cells (Figure 1C, left panel). There was more lactate production in the culture supernatants of the EBV-infected B cells (Figure 1C, right panel), so lactate-rich acidic conditions may contribute to adhesion and morphological changes of EBV-immortalized LCL cells.

LA acid promotes cell adhesion, morphological changes, and motility of

EBV-immortalized B cells

Cell viability data suggest that (Figure 2A) LA slightly promoted the proliferation of EBV-infected and uninfected B cells at ≤10 mM, and it gradually inhibited proliferation at increasing concentrations after 20 mM. EBV-infected B-lymphoma cells were more sensitive than uninfected B-lymphoma cells to higher concentrations of LA. Lower LA concentrations induced cell adhesion and spindle-like morphological changes (similar to LCL cells in long-term culture, Figure 1B) and S-phase arrest of EBV-infected (Figure 2B and C).

The data show that lactate (pH 6.8) caused significant cell adhesion and morphological changes (Figure 2C), and EBV-positive Burkitt lymphoma cells (EBV-infected Akata cells) treated with LA did not respond in the same way (data not shown). Thus, LA-induced cell adhesion and morphological changes of EBV-infected B lymphoblastic cells may be exclusively latency III-type dependent.

To address whether adhesive EBV-infected B cells induced by LA can continue to proliferate after attachment, we used a cell-attached counter technique of electron flow. Figure 2D results show that LA significantly induced cell adhesion and proliferation of EBV-immortalized LCL cells, but not in the mock, lactate sodium, or acidic-treated groups. In contrast, except for increased attachment, LA treatment did not significantly impair the cell growth of unattached EBV-infected B cells, EBV episome DNA copy, or virion production (Figure 3A and B). The lactate sodium-treated group had induced

272 EBV episome replication and some release of virion particles.

273 To confirm that LA enhances EBV-immortalized B cells adhesiveness, a
274 cell adhesion assay using different doses of fibronectin was performed in cells
275 treated with/without LA. Data show that EBV-immortalized LCL1 and B95.8
276 cells adhered to fibronectin after LA treatment, and adherent cells increased in
277 a dose-dependent manner relative to untreated cells (Figure 4A). To
278 investigate whether LA induced motility of adherent B cells, Transwell assays
279 were performed and B95.8 and LCL treated with LA had significantly more
280 migration and invasiveness compared to the untreated controls ($p < 0.01$,
281 Figure 4B and C).

282 **Gene profiles of EBV-infected B cells in response to LA**

283 We used cellular and viral RNA deep sequencing analysis of
284 EBV-immortalized B cells in the presence/absence of LA. More than 6,721
285 genes from 50 unique functional pathways were differentially expressed in
286 EBV-infected B cells after LA treatment (Figure 5A). Among the 50 functional
287 pathways, at least five regulatory pathways (187 genes involved) of cellular
288 processes and environmental information processing (See Figure 5A) were
289 associated with morphology and cell malignancy (Figure 5A). Moreover, the
290 functional pathway of EBV infection (a human disease category) was
291 confirmed, suggesting viral infection (Figure 5A). Interestingly, EBV gene
292 expression profile analysis revealed that LA not only significantly reduced the
293 transcription of LMP1, LMP2A, and BNLF2A, but it also enhanced the

294 expression of many viral latent and lytic genes as shown in Figure 5B. This
295 indicates that the life cycle switch from latency to lytic replication is not the key
296 response of EBV to LA, supporting the fact that no significant production of
297 virion particles by LA treatment was observed (Figure 3B).

298 After randomly selecting nine genes related to ECM regulation
299 with/without significant changes, we verified them using quantitative PCR.
300 Consistently, the expression of ECM-related molecules, including CD44, matrix
301 metalloprotein (MMP7 and MMP9), and collagen 1A (COL1A), was increased
302 in EBV-immortalized B cells in the presence of LA (Figure 5C, D).

303 **LA globally inhibits expression of EBV miRNAs**

304 We next investigated whether the cell adhesion of EBV-immortalized B
305 cells is attributable to the miRNA expression changes of EBV in response to
306 LA. Using viral miRNA deep sequencing followed by integrative analysis, we
307 assessed paired cellular mRNA and viral miRNA expression profiles related to
308 LA and 13 of 48 miRNAs encoded by EBV were confirmed in EBV-infected B
309 cells. Most EBV miRNAs were inhibited by LA, and the miR-BHRF1 cluster
310 (miR-BHRF1-1, miR-BHRF1-2-5p, miR-BHRF1-2-3p, and miR-BHRF1-3) and
311 miR-BART1-5p had more than two-fold expression changes (Figure 6A). Next,
312 we selected and verified miRNAs of the miR-BHRF1 cluster and partial
313 miR-BART using quantitative PCR in LCL and B95.8 cells treated with LA as
314 indicated. miR-BHRF1-1, miR-BHRF1-3, and miR-BART1-5p were
315 significantly reduced in the presence of LA (Figure 6B), suggesting a role of the

316 miR-BHRF1 cluster in response to LA.

317 To elucidate candidate targets and potential biological functions of
318 miR-BHRF1-1, miR-BHRF1-3, miR-BHRF1-2-3p, miR-BHRF1-2-5p, and
319 miR-BART1-5p, interrelated pairs of abnormal miRNA-abnormal target mRNA
320 from deep-sequencing data were explored, and we found no target gene for
321 miR-BHRF1-2-3p, but there were genes targeted by the other four
322 LA-associated EBV miRNAs in a functional network with miR-BHRF1-1-target
323 genes as the core (Figure 6C, Table 2). Signaling pathway analysis revealed
324 that miR-BHRF1-1 exclusively disrupts ECM-associated genes involved in
325 several cellular processes, as shown in Figure 6D.

326 **LA upregulates the TGF-β signaling pathway**

327 We measured SMAD3 and JUN (two components of TGF-β signaling) in
328 the core of four EBV miRNA target gene networks in response to LA (Figure
329 6C). Data show that the expressions of JUN and SMAD3 were enhanced in a
330 dose-dependent manner in EBV-immortalized B cells after LA stimulation, but
331 there were no significant changes in the expression in the TGF-β receptor
332 TGFBR1 (Figure 7A). Consistent with this trend, the increased expression of
333 the extracellular matrix protein, COL1A, was measured in EBV-infected cells
334 treated with LA (Figure 7A). Data from quantitative PCR analysis showed that
335 LA enhances the transcription of SMAD3 and JUN in EBV-immortalized B cells
336 (Figure 7B).

337 To ascertain whether the LA-induced expression of SMAD3 and JUN is

associated with interactions between miR-BHRF1-1 and its target sequences within the 3‘-UTR of each gene, 3‘-UTR regions of SMAD3 and JUN were assessed bioinformatically. The 3‘-UTR regions of SMAD3 and JUN contained a complementary site with the seed sequence of miR-BHRF1-1 at the nucleotide positions 3434-3452 and 913-934, respectively (Figure 7C, top panel). To clarify whether SMAD3 and JUN are direct cellular targets of miR-BHRF1-1, we used a luciferase reporter assay in HEK293 cells with wild-type and seed mutants of SMAD3 or JUN 3’-UTR-driven luciferase reporters in the presence/absence of miR-BHRF1-1 mimics. Luciferase activity of wild-type SMAD3 and JUN 3‘-UTR, but not mutants, was significantly reduced upon the co-expression of miR-BHRF1-1 mimics. There was no change in luciferase activity with the non-specific control miRNA mimic (Figure 7C, bottom panel).

Overexpression of miR-BHRF1-1 blocks LA-induced effect of EBV-infected B cells

To validate whether the inhibition of miR-BHRF1-1 by LA physiologically contributes to cell adhesion and motility of EBV-infected B cells, Transwell migration and invasion assays were performed using EBV-infected B cells transfected with miR-BHRF1-1 or control mimics with LA. In contrast to the untransfected (mock) controls, LA-induced cell adhesion and motility of the EBV-infected LCL and B95.8 cells were significantly blocked by the introduction of miR-BHRF1-1 compared to the control mimics (Figure 8A and

B). Immunoblotting experiments confirmed that miR-BHRF1-1 inhibits the LA-induced expression of SMAD3, JUN, and COL1A of the TGF-β signaling pathway in LCL and B95.8 cell lines (Figure 8C). To validate the potential role of miR-BHRF1-1 in LA-mediated cell adhesion and proliferation of EBV-infected B cells, similar assays were performed by introducing miR-BHRF1-1 mimics into the EBV-infected LCL cells with LA treatment, and miR-BHRF1-1 reduced the cell proliferation of attached EBV-infected B cells induced by LA (Figure 8D). Thus, miR-BHRF1-1 may contribute to cell adhesion, proliferation, and motility of EBV-infected B cells in response to LA.

370 **DISCUSSION**

371 Cancer cells adapt to changing environmental conditions to facilitate
372 continuous tumor growth. Changes in tumor metabolism contribute to
373 malignancy and (23) despite sufficient oxygen, tumor cells prefer aerobic
374 glycolysis to produce lactate (24). Thus, extracellular pH decreases
375 significantly and normal cells undergo apoptosis and malignant cells invade
376 the parenchyma to form an acidic microenvironment. Our findings suggest that
377 EBV infection induces significant upregulation of LDH-A and lactate, which
378 accumulates to create an acidic stress signal in the extracellular
379 microenvironment. This permits the selection of more aggressive B cells that
380 adhere, proliferate, and move via enhanced expressions of extracellular
381 matrix-associated genes, including SMAD3, JUN, and COL1A. In contrast, LA
382 accumulation secreted in the extracellular environment modulates LDH
383 expression and LA production in a feedback loop to enhance EBV-infected B
384 lymphoblastic cell survival (Figure 9). Then, LA-associated adhesion and
385 proliferation of EBV-infected B cells is at least partially due to the inhibition of
386 EBV-encoded miRNA, including the miR-BHRF1 cluster (Figure 9).

387 Consistent with previous observations in many cancers (9, 24, 25), LDH
388 was elevated in B cells by EBV infection and in EBV-positive B-cell lymphoma
389 cells. However, previous studies suggest that EBV encodes LMP1 to
390 upregulate anaerobic glycolysis (20, 21), and c-myc induces LDH-A
391 expression (26), but whether EBV upregulates c-Myc to induce LDH-A

392 expression or is directly induced by LMP1 is not clear. Interestingly, several
393 reports show that an acidic microenvironment induces apoptosis of normal
394 cells (22, 27), and EBV-infected B lymphoblastic cells, particularly EBV latency
395 III, are more sensitive than uninfected B-lymphoma cells in response to LA
396 treatment (IC_{50EBV+} = 40mM vs IC_{50EBV-} = 70mM), which may provide select
397 pressure against EBV-infected B cells with low LDH-A. This may explain, to
398 some extent, why EBV-positive B lymphoma is more malignant than
399 EBV-negative B lymphoma (28, 29).

400 Increasing evidence indicates that the dysregulation of microRNAs
401 (miRNAs) are characteristic of diverse human cancers (30). EBV is the first
402 human oncogenic virus reported to encode miRNAs (31) and to date, 25
403 EBV-miRNA precursors containing 48 mature miRNAs have been identified
404 within two regions of the EBV genome (32). One is the miR-BHRF1 cluster that
405 encodes three miRNA precursors and generates four mature miRNAs. The
406 other is the miR-BART cluster that contains 22 miRNA precursors and
407 produces 44 mature miRNAs. These EBV-encoded miRNAs have also been
408 shown to be important regulators for host–pathogen interactions and viral
409 carcinogenesis (33). In different host cells, the expression profile of these viral
410 miRNAs could be different and may serve as biomarkers for EBV-associated
411 diseases (34-37). Consistent with previous studies, which showed that the
412 expression of miRNA from the miR-BHRF1 cluster was relatively restricted to
413 lytic and latency III phases of EBV-infected B lymphoma cells (36, 38-42), we

414 also observed that the miR-BHRF1 cluster is highly expressed in
415 EBV-immortalized LCL cells and responds to LA treatment. In contrast,
416 miR-BART induces tumor metastasis by regulating PTEN-dependent
417 pathways and acts as a biomarker in nasopharyngeal carcinoma (33, 43),
418 suggesting a tissue-specific pathogenic role of the miR-BHRF1 cluster that
419 regulates the development of EBV-associated B lymphoma malignancies in
420 response to LA. Although several studies indicate that the EBV miRNA locus
421 contributes to B cell transformation during primary EBV infection (44-46), we
422 observed that the expression of most of EBV miRNAs are downregulated in
423 the presence of LA, indicating that the EBV miRNA cluster plays different roles
424 in the establishment and maintenance of viral latency, especially in response
425 to LA, but how LA suppresses expression of EBV miRNAs warrants more study.
426 In addition, we also observed that the expression of viral genes LMP1, EBNA1,
427 2, and 3A/C in EBV-infected B cells treated with LA were similar to B cells
428 primarily infected with the miR-BHRF1-deleted EBV mutant. Because latent
429 proteins EBNA1, 2, and 3A/C contribute to deregulating CD8 T-cell responses
430 against EBV-infected cells (47) and excess LMP1 is toxic to infected B cells
431 (48), the relative excess of latent proteins EBNA1, 2, and 3A/C and reduced
432 LMP1 induced by LA may facilitate viral immune evasion and host cell survival.
433 Moreover, given the role of LMP1 on the induction of anaerobic glycolysis (20,
434 21), LA-mediated inhibition of LMP1 expression may provide a potential
435 explanation for EBV control at the extracellular LA level in a feedback manner.

We report that LA alters the phenotype of EBV-infected B cells by regulating the ECM expression in a TGF-β pathway-dependent manner. Also, LA suppresses expression of EBV miRNAs (particularly miR-BHRF1-1), enhanced JUN and SMAD3 and increased EBV-infected B cell adhesion, proliferation, and motility via upregulating the ECM-associated molecules COL1A, MMP-7, and MMP-9. Of these, JUN was highly associated with adhesion of EBV-infected B cells to the extracellular matrix *in vitro*, and this agrees with data regarding DLBCL (49).

An acidic environment is toxic to normal cells and can inhibit the immune response to viral antigens, and LA drives rapid growth of cancer cells and promotes replication and dissemination of the EBV virion formation in an acidic microenvironment. Results from RNA deep sequencing analysis suggest that LMP1 and LMP2A expressions are inhibited but EBNA1, 2, 3A/C, and Rta are enhanced by LA, which individually contribute to maintaining EBV latency or initiating lytic replication. Whether LA contributes to switching EBV from the latent to the lytic state is not clear.

Of note, despite lactate uptake and utilization being fuel in endothelial cells (50), its effects on B cells is not clear. We showed that LA promotes cell adhesion, proliferation, and motility of EBV-infected B cells, particular for viral latency III but not for other types, suggesting a role of lactate in the progression of EBV-driven B lymphoma malignancy. Thus, we offer evidence that the miR-BHRF1-SMAD3-JUN axis mediates cell adhesion and

458 proliferation of EBV-associated B lymphoblastic cells within the acidic
459 microenvironment, and it contributes to B lymphoma growth and dissemination,
460 which may be useful biomarkers and targets for intervention during the early
461 neoplastic formation of EBV-associated B lymphoma.

462 ACKNOWLEDGMENTS

463 We are grateful to Dr. Xiaozheng Liang from Shanghai Pasteur Institute for
464 providing reagents. This work is supported by the National Key Research and
465 Development Program of China (2016YFC1200400 to QC), and the National
466 Natural Science Foundation of China (81471930, 81672015 to QC; 81402542,
467 81772166 to FW, 81502738 to XM, 81501739 to CZ). FW is a scholar of Pujiang
468 Talents in Shanghai. QC is a scholar of New Century Excellent Talents in
469 University of China.

REFERENCES

1. **Warburg O.** 1956. On the origin of cancer cells. Science **123:**309-314.
2. **DeBerardinis RJ, Lum JJ, Hatzivassiliou G, Thompson CB.** 2008. The biology of cancer: metabolic reprogramming fuels cell growth and proliferation. Cell metabolism **7:**11-20.
3. **Gladden LB.** 2004. Lactate metabolism: a new paradigm for the third millennium. The Journal of physiology **558:**5-30.
4. **Schurr A, West CA, Rigor BM.** 1988. Lactate-supported synaptic function in the rat hippocampal slice preparation. Science **240:**1326-1328.
5. **De Saedeleer CJ, Copetti T, Porporato PE, Verrax J, Feron O, Sonveaux P.** 2012. Lactate activates HIF-1 in oxidative but not in Warburg-phenotype human tumor cells. PloS one **7:**e46571.
6. **Bonuccelli G, Tsirigos A, Whitaker-Menezes D, Pavlides S, Pestell RG, Chiavarina B, Frank PG, Flomenberg N, Howell A, Martinez-Outschoorn UE, Sotgia F, Lisanti MP.** 2010. Ketones and lactate "fuel" tumor growth and metastasis: Evidence that epithelial cancer cells use oxidative mitochondrial metabolism. Cell cycle **9:**3506-3514.
7. **Hirschhaeuser F, Sattler UG, Mueller-Klieser W.** 2011. Lactate: a metabolic key player in cancer. Cancer research **71:**6921-6925.
8. **Goodwin ML, Gladden LB, Nijsten MW, Jones KB.** 2014. Lactate and cancer: revisiting the warburg effect in an era of lactate shuttling. Frontiers in nutrition **1:**27.
9. **Liu R, Cao J, Gao X, Zhang J, Wang L, Wang B, Guo L, Hu X, Wang Z.** 2016. Overall survival of cancer patients with serum lactate dehydrogenase greater than 1000 IU/L. Tumour biology : the journal of the International Society for Oncodevelopmental Biology and Medicine **37:**14083-14088.
10. **Wang J, Wang H, Liu A, Fang C, Hao J, Wang Z.** 2015. Lactate dehydrogenase A negatively regulated by miRNAs promotes aerobic glycolysis and is increased in colorectal cancer. Oncotarget **6:**19456-19468.
11. **Kutok JL, Wang F.** 2006. Spectrum of Epstein-Barr virus-associated diseases. Annual review of pathology **1:**375-404.
12. **Yuan J, Cahir-McFarland E, Zhao B, Kieff E.** 2006. Virus and cell RNAs expressed during Epstein-Barr virus replication. Journal of virology **80:**2548-2565.
13. **Ersing I, Nobre L, Wang LW, Soday L, Ma Y, Paulo JA, Narita Y, Ashbaugh CW, Jiang C, Grayson NE, Kieff E, Gygi SP, Weekes MP, Gewurz BE.** 2017. A Temporal Proteomic Map of Epstein-Barr Virus Lytic Replication in B Cells. Cell reports **19:**1479-1493.
14. **Grywalska E, Rolinski J.** 2015. Epstein-Barr virus-associated lymphomas. Seminars in oncology **42:**291-303.
15. **Zhu C, Zhu Q, Wang C, Zhang L, Wei F, Cai Q.** 2016. Hostile takeover: Manipulation of HIF-1 signaling in pathogen-associated cancers (Review). International journal of oncology **49:**1269-1276.
16. **Darekar S, Georgiou K, Yurchenko M, Yenamandra SP, Chachami G, Simos G, Klein G, Kashuba E.** 2012. Epstein-Barr virus immortalization of human B-cells leads to stabilization of hypoxia-induced factor 1 alpha, congruent with the Warburg effect. PloS one **7:**e42072.
17. **Kondo S, Seo SY, Yoshizaki T, Wakisaka N, Furukawa M, Joab I, Jang KL, Pagano JS.** 2006. EBV latent membrane protein 1 up-regulates hypoxia-inducible factor 1alpha through Siah1-mediated down-regulation of prolyl hydroxylases 1 and 3 in nasopharyngeal epithelial

cells. Cancer research **66:**9870-9877.

18. **Wakisaka N, Kondo S, Yoshizaki T, Murono S, Furukawa M, Pagano JS.** 2004. Epstein-Barr virus latent membrane protein 1 induces synthesis of hypoxia-inducible factor 1 alpha. Molecular and cellular biology **24:**5223-5234.

19. **Jiang JH, Wang N, Li A, Liao WT, Pan ZG, Mai SJ, Li DJ, Zeng MS, Wen JM, Zeng YX.** 2006. Hypoxia can contribute to the induction of the Epstein-Barr virus (EBV) lytic cycle. Journal of clinical virology : the official publication of the Pan American Society for Clinical Virology **37:**98-103.

20. **Xiao L, Hu ZY, Dong X, Tan Z, Li W, Tang M, Chen L, Yang L, Tao Y, Jiang Y, Li J, Yi B, Li B, Fan S, You S, Deng X, Hu F, Feng L, Bode AM, Dong Z, Sun LQ, Cao Y.** 2014. Targeting Epstein-Barr virus oncoprotein LMP1-mediated glycolysis sensitizes nasopharyngeal carcinoma to radiation therapy. Oncogene **33:**4568-4578.

21. **Sommermann TG, O'Neill K, Plas DR, Cahir-McFarland E.** 2011. IKKbeta and NF-kappaB transcription govern lymphoma cell survival through AKT-induced plasma membrane trafficking of GLUT1. Cancer research **71:**7291-7300.

22. **Pike SE, Markey SP, Ijames C, Jones KD, Tosato G.** 1991. The role of lactic acid in autocrine B-cell growth stimulation. Proceedings of the National Academy of Sciences of the United States of America **88:**11081-11085.

23. **McFate T, Mohyeldin A, Lu H, Thakar J, Henriques J, Halim ND, Wu H, Schell MJ, Tsang TM, Teahan O, Zhou S, Califano JA, Jeoung NH, Harris RA, Verma A.** 2008. Pyruvate dehydrogenase complex activity controls metabolic and malignant phenotype in cancer cells. The Journal of biological chemistry **283:**22700-22708.

24. **Kim YR, Kim SJ, Cheong JW, Yang DH, Lee H, Eom HS, Sung YO, Kim HJ, Kang HJ, Lee WS, Park Y, Yang WI, Min YH, Kim JS.** 2016. The different roles of molecular classification according to upfront autologous stem cell transplantation in advanced-stage diffuse large B cell lymphoma patients with elevated serum lactate dehydrogenase. Annals of hematology **95:**1491-1501.

25. **Zha X, Wang F, Wang Y, He S, Jing Y, Wu X, Zhang H.** 2011. Lactate dehydrogenase B is critical for hyperactive mTOR-mediated tumorigenesis. Cancer research **71:**13-18.

26. **Shim H, Dolde C, Lewis BC, Wu CS, Dang G, Jungmann RA, Dalla-Favera R, Dang CV.** 1997. c-Myc transactivation of LDH-A: implications for tumor metabolism and growth. Proceedings of the National Academy of Sciences of the United States of America **94:**6658-6663.

27. **Goetze K, Walenta S, Ksiazkiewicz M, Kunz-Schughart LA, Mueller-Klieser W.** 2011. Lactate enhances motility of tumor cells and inhibits monocyte migration and cytokine release. International journal of oncology **39:**453-463.

28. **Block JB, Bronson WR, Bell WR.** 1966. Metabolic abnormalities of lactic acid in Burkitt-type lymphoma with malignant effusions. Annals of internal medicine **65:**101-108.

29. **Boag JM, Beesley AH, Firth MJ, Freitas JR, Ford J, Hoffmann K, Cummings AJ, de Klerk NH, Kees UR.** 2006. Altered glucose metabolism in childhood pre-B acute lymphoblastic leukaemia. Leukemia **20:**1731-1737.

30. **Esquela-Kerscher A, Slack FJ.** 2006. Oncomirs - microRNAs with a role in cancer. Nature reviews. Cancer **6:**259-269.

31. **Pfeffer S, Zavolan M, Grasser FA, Chien M, Russo JJ, Ju J, John B, Enright AJ, Marks D, Sander C, Tuschl T.** 2004. Identification of virus-encoded microRNAs. Science **304:**734-736.

32. **Kuzembayeva M, Hayes M, Sugden B.** 2014. Multiple functions are mediated by the miRNAs of Epstein-Barr virus. Current opinion in virology **7:**61-65.

33. **Cai L, Ye Y, Jiang Q, Chen Y, Lyu X, Li J, Wang S, Liu T, Cai H, Yao K, Li JL, Li X.** 2015. Epstein-Barr virus-encoded microRNA BART1 induces tumour metastasis by regulating PTEN-dependent pathways in nasopharyngeal carcinoma. Nature communications **6:**7353.

34. **Malterer G, Dolken L, Haas J.** 2011. The miRNA-targetome of KSHV and EBV in human B-cells. RNA biology **8:**30-34.

35. **Qiu J, Cosmopoulos K, Pegtel M, Hopmans E, Murray P, Middeldorp J, Shapiro M, Thorley-Lawson DA.** 2011. A novel persistence associated EBV miRNA expression profile is disrupted in neoplasia. PLoS pathogens **7:**e1002193.

36. **Xia T, O'Hara A, Araujo I, Barreto J, Carvalho E, Sapucaia JB, Ramos JC, Luz E, Pedroso C, Manrique M, Toomey NL, Brites C, Dittmer DP, Harrington WJ, Jr.** 2008. EBV microRNAs in primary lymphomas and targeting of CXCL-11 by ebv-mir-BHRF1-3. Cancer research **68:**1436-1442.

37. **Wang YF, He DD, Liang HW, Yang D, Yue H, Zhang XM, Wang R, Li B, Yang HX, Liu Y, Chen Y, Duan YX, Zhang CY, Chen X, Fu J.** 2017. The identification of up-regulated ebv-miR-BHRF1-2-5p targeting MALT1 and ebv-miR-BHRF1-3 in the circulation of patients with multiple sclerosis. Clinical and experimental immunology **189:**120-126.

38. **Skalsky RL, Corcoran DL, Gottwein E, Frank CL, Kang D, Hafner M, Nusbaum JD, Feederle R, Delecluse HJ, Luftig MA, Tuschl T, Ohler U, Cullen BR.** 2012. The viral and cellular microRNA targetome in lymphoblastoid cell lines. PLoS pathogens **8:**e1002484.

39. **Li J, Callegari S, Masucci MG.** 2017. The Epstein-Barr virus miR-BHRF1-1 targets RNF4 during productive infection to promote the accumulation of SUMO conjugates and the release of infectious virus. PLoS pathogens **13:**e1006338.

40. **Li Z, Chen X, Li L, Liu S, Yang L, Ma X, Tang M, Bode AM, Dong Z, Sun L, Cao Y.** 2012. EBV encoded miR-BHRF1-1 potentiates viral lytic replication by downregulating host p53 in nasopharyngeal carcinoma. The international journal of biochemistry & cell biology **44:**275-279.

41. **Ma J, Nie K, Redmond D, Liu Y, Elemento O, Knowles DM, Tam W.** 2016. EBV-miR-BHRF1-2 targets PRDM1/Blimp1: potential role in EBV lymphomagenesis. Leukemia **30:**594-604.

42. **Poling BC, Price AM, Luftig MA, Cullen BR.** 2017. The Epstein-Barr virus miR-BHRF1 microRNAs regulate viral gene expression in cis. Virology **512:**113-123.

43. **Zhang G, Zong J, Lin S, Verhoeven RJ, Tong S, Chen Y, Ji M, Cheng W, Tsao SW, Lung M, Pan J, Chen H.** 2015. Circulating Epstein-Barr virus microRNAs miR-BART7 and miR-BART13 as biomarkers for nasopharyngeal carcinoma diagnosis and treatment. International journal of cancer **136:**E301-312.

44. **Seto E, Moosmann A, Gromminger S, Walz N, Grundhoff A, Hammerschmidt W.** 2010. Micro RNAs of Epstein-Barr virus promote cell cycle progression and prevent apoptosis of primary human B cells. PLoS pathogens **6:**e1001063.

45. **Feederle R, Linnstaedt SD, Bannert H, Lips H, Bencun M, Cullen BR, Delecluse HJ.** 2011. A viral microRNA cluster strongly potentiates the transforming properties of a human herpesvirus. PLoS pathogens **7:**e1001294.

46. **Feederle R, Haar J, Bernhardt K, Linnstaedt SD, Bannert H, Lips H, Cullen BR, Delecluse HJ.** 2011. The members of an Epstein-Barr virus microRNA cluster cooperate to transform B

lymphocytes. Journal of virology **85:**9801-9810.

47. **Rickinson AB, Callan MF, Annels NE.** 2000. T-cell memory: lessons from Epstein-Barr virus infection in man. Philosophical transactions of the Royal Society of London. Series B, Biological sciences **355:**391-400.

48. **Hammerschmidt W, Sugden B.** 1989. Genetic analysis of immortalizing functions of Epstein-Barr virus in human B lymphocytes. Nature **340:**393-397.

49. **Blonska M, Zhu Y, Chuang HH, You MJ, Kunkalla K, Vega F, Lin X.** 2015. Jun-regulated genes promote interaction of diffuse large B-cell lymphoma with the microenvironment. Blood **125:**981-991.

50. **Krutzfeldt A, Spahr R, Mertens S, Siegmund B, Piper HM.** 1990. Metabolism of exogenous substrates by coronary endothelial cells in culture. Journal of molecular and cellular cardiology **22:**1393-1404.

616 **TABLES**

617 **Table 1**. Primers for PCR and oligos used in this study.

Target	Primer/Oligo sequence	Product (bp)
LDH-A	Sense: 5'- GGCCTCTGCCATCAGTATCT -3' Antisense : 5'- GCCGTGATAATGACCAGCTT -3'	189
SMAD3	Sense : 5'- GGAGAAATGGTGCGAGAAGG -3' Antisense : 5'- GAAGGCGAACTCACACAGC -3'	259
JUN	Sense : 5'- AAGTAAGAGTGCGGGAGGCA -3' Antisense : 5'- GGGCATCGTCATAGAAGGTCG -3'	268
CD44	Sense: 5'-GACAAGTTTTGGTGGCACG-3' Antisense: 5'-CACGTGGAATACACCTGCAA-3'	105
COL1A1	Sense: 5'-AAGAGGAAGGCCAAGTCGAG-3' Antisense: 5'-CACACGTCTCGGTCATGGTA-3'	91
ELN	Sense: 5'-GTCCTCCTGCTCCTGCTGT-3' Antisense: 5'GCCCCTGGATAAAAGACTCC-3'	101
FN1	Sense: 5'-CCATAAAGGGCAACCAAGAG-3' Antisense: 5'-ACCTCGGTGTTGTAAGGTGG-3'	91
PRG2	Sense: 5'-TGAGCTGGTCCCAGCCAGCA-3' Antisense: 5'-TCCTCCTCAAGGAGTAGTAG-3'	240
FNDC5	Sense: 5'-GGCTCCACTCATTGTCTTGT-3' Antisense: 5'-AGTGGTTATTGCTCTAAGT-3'	109
LAMA4	Sense: 5'-CCGCAGGGAAAGGCGGACCT-3'	180

	Antisense: 5'-ATTGGGGTGAGCCCCGCCAGC-3'	
MMP9	Sense: 5'-CTCTGGCAGCCCCTGGTCCTGG-3' Antisense: 5'-CCAGCTGCCTGTCGGTGAGAT-3'	127
MMP7	Sense: 5'-GGATGGTAGCAGTCTAGGGATTAACT-3' Antisense: 5'-AGGTTGGATACATCACTGCATTAG-3'	110
GAPDH	Sense : 5'- GTCAACGGATTTGGTCTGTATT -3' Antisense : 5'- AGTCTTCTGGGTGGCAGTGAT -3'	228
miR-BHRF1-1	5' AGCAAGAATAACCTGATCAGCCCCGGAGTT 3'	-
snU6	5' TGCTAATCTTCTCTG-TATCGT 3'	-

618

619 **Table 2**. List of potential genes targeted by the EBV miRNAs in response to lactate in LCL with significantly different expression.

miRNA	Target Genes	Description	Log2(fold change)
BHRF1-1	ATHL1	acid trehalase-like 1	1.400
	CCL22	chemokine (C-C motif) ligand 22	3.986
	CYTH3	cytohesin 3	1.195
	DAP	death-associated protein	1.1751
	DNAJC5B	DnaJ (Hsp40) homolog, subfamily C, member 5 beta	3.878
	DYX1C1-CCPG1	DYX1C1-CCPG1 readthrough (NMD candidate)	1.527
	EXD2	exonuclease 3'-5' domain containing 2	1.289
	FBXO27	F-box protein 27	7.288
	FLCN	Folliculin	1.430
	FLJ40852	uncharacterized LOC285962	4.527
	FOXO4	forkhead box O4	1.554
	FZD2	frizzled family receptor 2	2.162
	HEATR6	HEAT repeat containing 6	1.268
	HELZ2	helicase with zinc finger 2, transcriptional coactivator	1.632
	IRAK2	interleukin-1 receptor-associated kinase 2	1.968
	JUN	jun proto-oncogene	2.539
	LACTB	lactamase, beta	1.007
	MDFIC	MyoD family inhibitor domain containing	5.287
	NUDT16	nudix (nucleoside diphosphate linked moiety X)-type motif 16	1.134
	OBFC1	oligonucleotide/oligosaccharide-binding fold containing 1	1.480
	PHLDB3	pleckstrin homology-like domain, family B, member 3	1.471

	PLXNA1	plexin A1	2.501
	RAB11FIP5	RAB11 family interacting protein 5 (class I)	3.726
	RAB13	RAB13, member RAS oncogene family	1.698
	RNF41	ring finger protein 41	1.069
	RXRA	retinoid X receptor, alpha	2.477
	SFXN3	sideroflexin 3	2.017
	SLC27A1	solute carrier family 27 (fatty acid transporter), member 1	1.431
	SMAD3	SMAD family member 3	1.128
	STK16	serine/threonine kinase 16	1.293
	TFE3	transcription factor binding to IGHM enhancer 3	1.443
	TMEM104	transmembrane protein 104	1.178
	TOM1L2	target of myb1-like 2 (chicken)	1.745
BHRF1-2-5p	CREBRF	CREB3 regulatory factor	1.694
	NPHP3-ACAD11	NPHP3-ACAD11 readthrough	1.538
	PDGFD	platelet derived growth factor D	1.522
	PLEKHM3	pleckstrin homology domain containing, family M, member 3	1.508
	STK10	serine/threonine kinase 10	1.654
BHRF1-2-3p	Unknown		
BHRF1-3	BTN3A1	butyrophilin, subfamily 3, member A1	1.689
	CBX4	chromobox homolog 4	2.512
	DUSP28	dual specificity phosphatase 28	1.012
	DYX1C1-CCPG1	DYX1C1-CCPG1 readthrough (NMD candidate)	1.527
	ENTPD1-AS1	ENTPD1 antisense RNA 1	1.578
	GNG7	guanine nucleotide binding protein (G protein), gamma 7	1.578

	LOC100506023	uncharacterized LOC100506023	1.831	620
	NUAK2	NUAK family, SNF1-like kinase, 2	1.068	
	PARS2	prolyl-tRNA synthetase 2, mitochondrial (putative)	1.070	
	PLXNA1	plexin A1	2.501	
	SPNS3	spinster homolog 3 (Drosophila)	4.995	
	TANC2	tetratricopeptide repeat, ankyrin repeat and coiled-coil containing 2	1.609	
	ZNF524	zinc finger protein 524	2.290	
BART1-5p	C1RL	complement component 1, r subcomponent-like	2.460	
	CASP10	caspase 10, apoptosis-related cysteine peptidase	1.000	
	CD68	CD68 molecule	1.438	
	CRTC3	CREB regulated transcription coactivator 3	1.210	
	DLG3	discs, large homolog 3 (Drosophila)	1.420	
	DYRK1B	dual-specificity tyrosine-(Y)-phosphorylation regulated kinase 1B	2.249	
	ENTPD1-AS1	ENTPD1 antisense RNA 1	2.153	
	FAM109A	family with sequence similarity 109, member A	1.306	
	FAM115C	family with sequence similarity 115, member C	5.170	
	FAM131A	family with sequence similarity 131, member A	2.320	
	KCTD15	potassium channel tetramerisation domain containing 15	3.978	
	PDZD7	PDZ domain containing 7	3.515	
	SLC35E1	solute carrier family 35, member E1	1.036	
	SMDT1	single-pass membrane protein with aspartate-rich tail 1	1.175	
	TOLLIP	toll interacting protein	1.188	
	TREML2	triggering receptor expressed on myeloid cells-like 2	1.112	
	ZNF264	zinc finger protein 264	1.334	

621 **FIGURE LEGENDS**

622 **Figure 1**. **LDH-A and LA production are elevated in EBV-immortalized B**
623 **lymphoblastic cells.** Cells were (**A**) established as described and karyotype
624 analysis of normal B cells, LCL1, and LCL2 cells showed that LCL1 cells were
625 similar to normal B cells but LCL2 cells had deletions. The left panels are
626 representative photographs of EBV-immortalized LCL cell lines derived from B
627 cells according to flow cytometry. (**B**) Representative photographs of adhesion
628 and morphological changes of EBV-immortalized lymphoblastic cells in
629 long-term culture medium. Adhesion and morphology of LCL1 and LCL2 cell
630 lines during exponential growth from panel A monitored at days 3 and 5
631 post-seed. White bar indicates 10 μM. Arrow indicates changes in cell
632 morphology. (**C**) High LDH-A expression and lactate production in
633 EBV-infected B-lymphoma cells. EBV-positive (B95.8, LCL1, and LCL2) and
634 negative (naïve B, BJAB, and Ramos) B cells were assessed for LDH-A mRNA
635 transcripts using quantitative PCR (Left panel). Lactate was measured in
636 culture supernatants after 24 h inoculation (right panel). Asterisks indicate
637 significant difference (*$p < 0.05$) between EBV-positive and -negative cells with
638 respect to LDH-A and lactate production.

639 **Figure 2**. **Distinct response of EBV-infected and uninfected B cells to LA.**
640 (**A**) Higher sensitivity of EBV-infected B cells in response to LA. B lymphoma
641 cells treated with LA as indicated and MTT assay data (mean ± SD) as relative
642 percent of untreated controls. (**B**) LA induces S phase arrest of EBV-infected B

643 cells. EBV-positive (LCL) or -negative (Ramos) cells were treated with of LA as
644 indicated and mean percentage of different phases (sub-G1, G1, S, G2/M)
645 from triplicate experiments are presented. (**C**) LA induces cell adhesion and
646 morphological changes of LCL1 and B95.8 and Ramos and BJAB B cells.
647 Representative photographs of cell morphology after treatment with LA, La-Na,
648 or pH 6.8 as indicated. Arrow indicates changes in cell morphology. (**D**)
649 Real-time monitoring of adhesion and proliferation of EBV-infected LCL cells
650 treated as indicated and assessed for adhesion and proliferation. Schematic of
651 xCELLIgence system for real-time monitoring of cell adhesion and proliferation
652 (right panel).

653 **Figure 3**. **LA promotes cell adhesion and proliferation of EBV-infected B**
654 **lymphoblastic cells.**

655 (**A**) LA promotes cell adhesion and proliferation of EBV-immortalized B
656 lymphoblastic cells after treatment as indicated. Measurement of attached
657 cells at 96 h post-seeding. (**B**) Relative copy number of EBV episome DNA
658 within cells and virion release in culture medium at 24 h treatment from panel A
659 quantified by quantitative PCR.

660 **Figure 4**. **LA enhances adhesion and motility of EBV-infected B**
661 **lymphoblastic cells.**

662 (**A**) LA enhances adhesion of EBV-infected B cells. Relative adhesion of
663 EBV-infected LCL and B95.8 B cells in presence/absence (mock) of LA as
664 indicated and measured using ELISA with fibronectin coating. Data are

665 representative of two independent experiments performed in triplicate. Motility
666 of EBV-infected LCL and B95.8 B cells in the presence/absence (mock) of 10
667 mM LA (LA), assessed by Transwell assays for cell migration (**B**) and invasion
668 (**C**). *In vitro* invasion assay performed using Transwell inserts coated with
669 Matrigel. Results are means + SD of triplicate cultures. Asterisks indicate
670 significant differences (*$p < 0.05$) between mock and LA-treated groups.

671 **Figure 5**. **LA significantly alters gene expression of EBV-infected B**
672 **lymphoblastic cells.**

673 (**A**) Functional clustering analysis of identified genes from EBV-infected B cells,
674 which expressions are significantly changed in response to LA. Gene number
675 of each functional signaling pathway with significant changes of expression
676 (>2-fold, $p < 0.01$) in LCL and B95.8 B cells after LA treatment were assessed
677 using RNA deep sequencing analysis and summarized from overlapping
678 genes for both cell lines (Left panel). Representative overview of gene number
679 with significant expression changes in EBV-infected B cells after LA treatment
680 (right panel). (**B**) Relative expression of EBV-encoded genes and (**C**)
681 extracellular matrix-related genes in EBV-infected B cells in the
682 presence/absence of LA from *panel A* are highlighted and represent
683 fold-change. (**D**) Gene expression in *panel C* was verified using quantitative
684 PCR in LCL and B95.8 B cells.

685 **Figure 6**. **LA inhibits expression of EBV-encoded miRNA.**

686 (**A**) Hierarchical clustering of EBV-miRNA profiling in response to LA. Analysis

of small RNA sequencing in EBV-infected LCL and B95.8 B cells revealed that the expression of miRNAs (5 out of 13) encoded by EBV is influenced by more than two-fold in the presence of LA. (**B**) Validation of representative miRNAs encoded by EBV in response to LA. Total RNA extracted from EBV-infected LCL and B95.8 B cells with/without LA treatment for 24 h assessed via quantitative PCR. (**C**) Hypothetical regulatory circuit of proteins targeted by five EBV-encoded miRNAs in response to LA. Core network with miR-BHRF1-1-targeted protein (red) interconnected hubs is displayed by dashed circles. Bigger nodes denote proteins that respond to LA and with more read counts according to RNA sequencing. (**D**) Functional clustering analysis of identified cellular genes targeted by miR-BHRF1-1 in EBV-infected B cells in response to LA.

Figure 7. LA activates gene expression of the TGF-β pathway in EBV-infected B lymphoblastic cells.

EBV-immortalized LCL cells were treated as indicated. (**A**) Immunoblotting for gene expression of the TGF-β pathway and extracellular matrix. (**B**) Relative expression of JUN and SMAD3 transcripts according to quantitative PCR analysis. Asterisk denotes significant difference (**$p < 0.01$). (**C**) miR-BHRF1-1 and its target sequences within the 3'-UTR of SMAD3 or JUN. Schematic representation of miR-BHRF1-1 putative binding site located at the 3'-UTR of SMAD3 or JUN. The highly conserved 9/10-bp (for SMAD3 and JUN, respectively) seed pair is underlined (*top panel*). The 293T cells were

co-transfected with reporter luciferase plasmids containing wild-type (WT) sequence or mutants (mut) with indicated miRNA precursors. Luciferase activity measured 24 h post transfection, and normalized against *Renilla* luciferase activity.

Figure 8. Introduction of miR-BHRF1-1 attenuates LA-induced cell adhesion, motility, and proliferation of EBV-infected B lymphoblastic cells.

LCL1 and B95.8 cells transfected as indicated and immunoblotted with antibodies. Mock cells were controls. LA-induced cell adhesion and motility of EBV-infected B cells measured by Transwell assay for cell migration (**A**) and invasion (**B**) as described. Representative images of cell motility (*left panels*), and relative quantification of cell clones in *right panels*. Results are means + SD of triplicate cultures. (**C**) Effect of miR-BHRF1-1 mimics on the expression of TGFBR1, SMAD3, JUN, and COL1A in the EBV-infected B lymphoblastic cells with LA treatment. (**D**) miR-BHRF1-1 inhibits the growth of attached EBV-infected B cells induced by LA.

Figure 9. Schematic of EBV (E)-immortalized B lymphoblastic cell adhesion and proliferation induced by LA. Production of LA induced by EBV infection is a selective signal that inhibits expression of viral miRNAs, particularly miR-BHRF1 for SMAD3 and JUN-mediated cell adhesion and feeds back to control LA secretion via inhibition of LDH-A expression for cell survival.

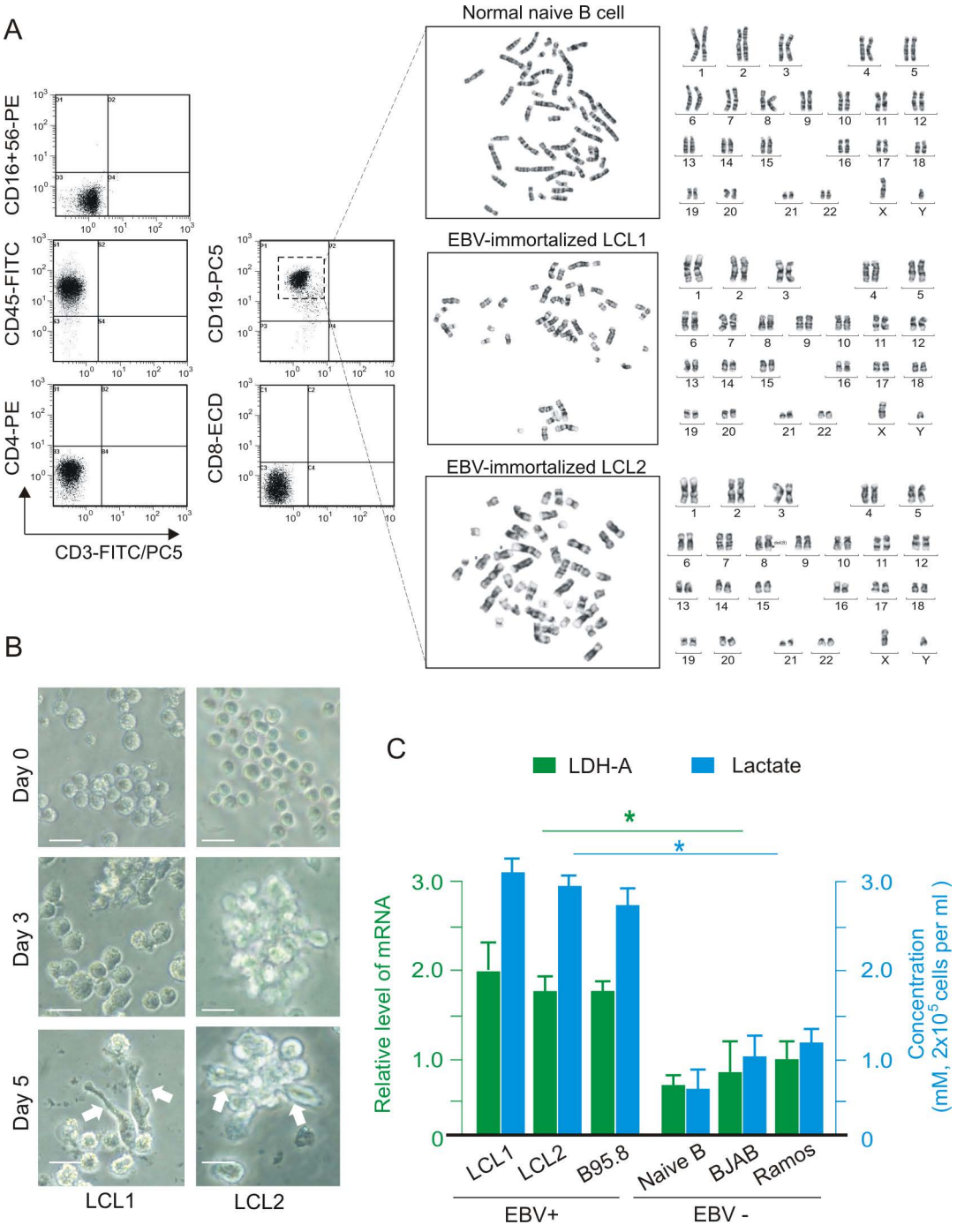

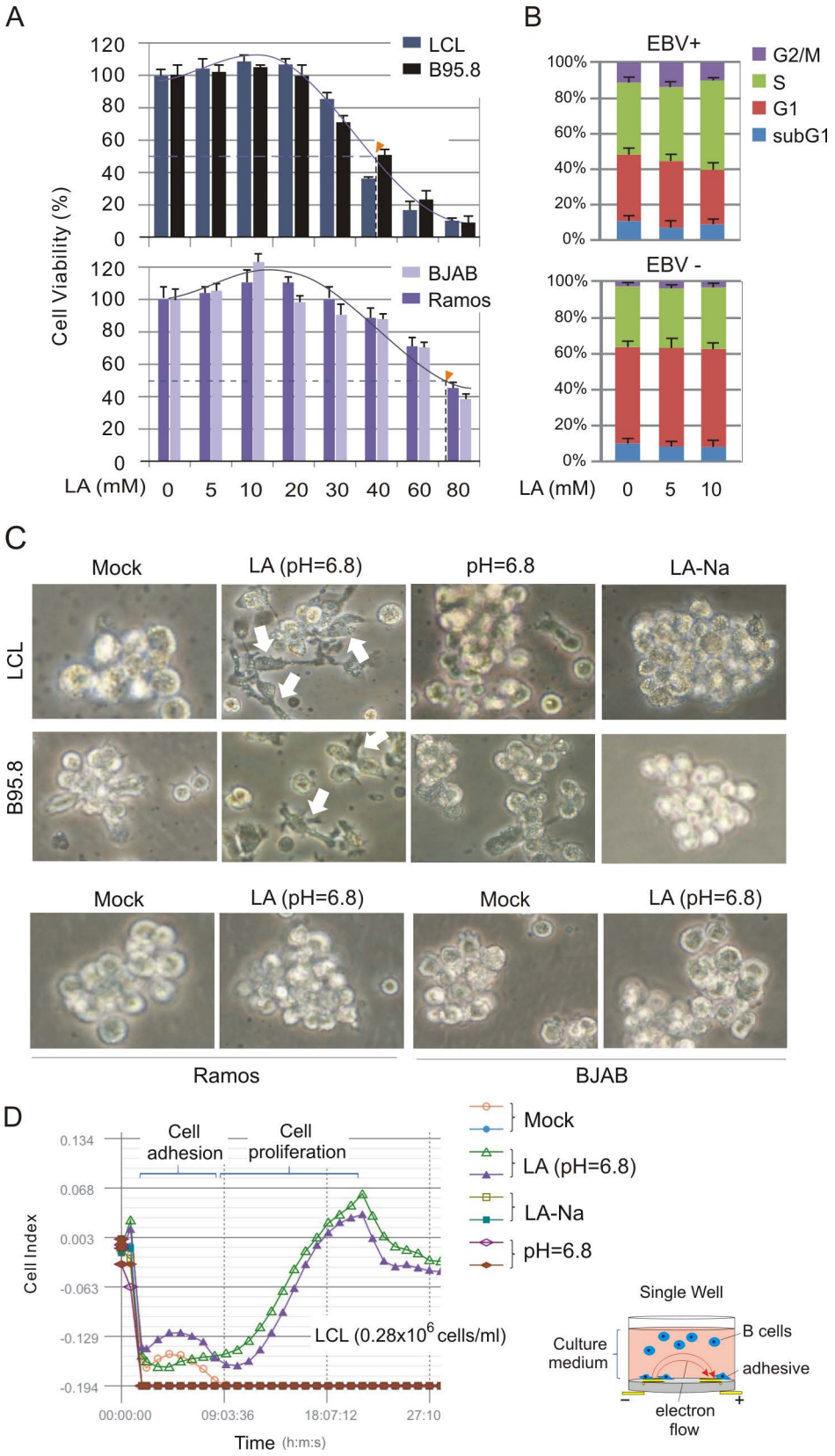

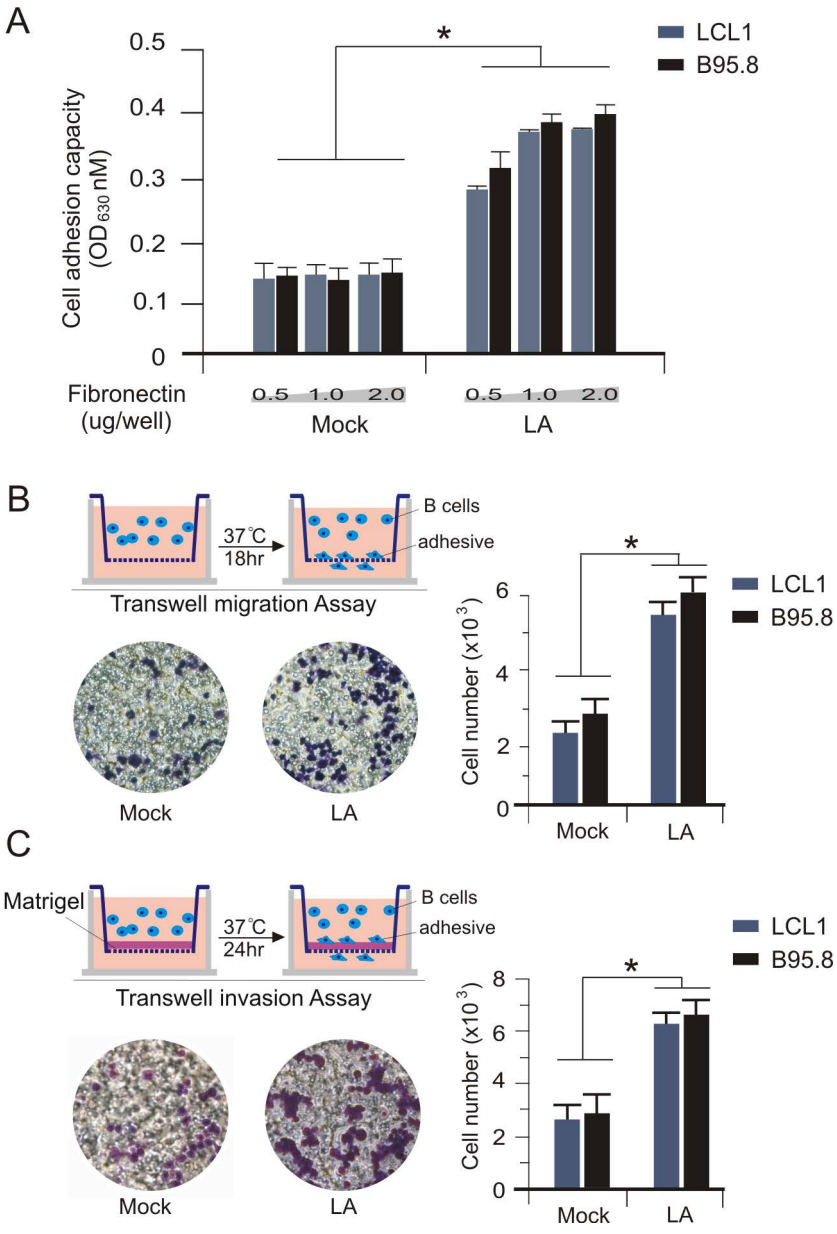

Journal of Virology